Acta Pharmacologica Sinica

www.nature.com/aps

ARTICLE

Dapagliflozin attenuates pressure overload-induced myocardial remodeling in mice via activating SIRT1 and inhibiting endoplasmic reticulum stress

Fang-fang Ren[1], Zuo-yi Xie[1], Yi-na Jiang[1], Xuan Guan[1], Qiao-ying Chen[1], Teng-fang Lai[2] and Lei Li[1]

Endoplasmic reticulum stress-mediated apoptosis plays a vital role in the occurrence and development of heart failure. Dapagliflozin (DAPA), a new type of sodium-glucose cotransporter 2 (SGLT2) inhibitor, is an oral hypoglycemic drug that reduces glucose reabsorption by the kidneys and increases glucose excretion in the urine. Studies have shown that DAPA may have the potential to treat heart failure in addition to controlling blood sugar. This study explored the effect of DAPA on endoplasmic reticulum stress-related apoptosis caused by heart failure. In vitro, we found that DAPA inhibited the expression of cleaved caspase 3, Bax, C/EBP homologous protein (CHOP), and glucose-regulated protein78 (GRP78) and upregulated the cardiomyoprotective protein Bcl-2 in angiotensin II (Ang II)-treated cardiomyocytes. In addition, DAPA promoted the expression of silent information regulator factor 2-related enzyme 1 (SIRT1) and suppressed the expression of activating transcription factor 4 (ATF4) and the ratios p-PERK/PERK and p-eIF2α/eIF2α. Notably, the therapeutic effect of DAPA was weakened by pretreatment with the SIRT1 inhibitor EX527 (10 μM). Simultaneous administration of DAPA inhibited the Ang II-induced transformation of fibroblasts into myofibroblasts and inhibited fibroblast migration. In summary, our present findings first indicate that DAPA could inhibit the PERK-eIF2α-CHOP axis of the ER stress response through the activation of SIRT1 in Ang II-treated cardiomyocytes and ameliorate heart failure development in vivo.

Keywords: DAPA; heart failure; ventricular remodeling; endoplasmic reticulum stress; SIRT1

Acta Pharmacologica Sinica (2022) 43:1721–1732; https://doi.org/10.1038/s41401-021-00805-2

INTRODUCTION

Heart failure is considered to be the final stage of heart disease [1]. Although various intervention targets have been explored in research on heart disease [2, 3], mortality and morbidity are still high, and this condition has become an increasingly serious public health problem [4]. The basic mechanism of the development of heart failure is ventricular remodeling [5]. Ventricular remodeling occurs through a series of complex molecular and cellular mechanisms that lead to changes in myocardial structure, function and phenotype, including pathological myocardial hypertrophy, excessive fibrosis, increased degradation of the cardiomyocyte outer base, and cardiomyocyte apoptosis. Studies have shown that cardiomyocytes are an indispensable component in the progression of heart failure [6] and that reducing the progression of heart failure is usually accompanied by apoptosis inhibition [7]. Therefore, inhibiting cardiomyocyte apoptosis is beneficial for the treatment of heart failure.

The endoplasmic reticulum is an organelle that stores Ca^{2+} and in which proteins are synthesized, folded and modified in eukaryotes. When subjected to stressors, misfolded and unfolded proteins accumulate in the endoplasmic reticulum lumen, and Ca^{2+} imbalance activates the unfolded protein response and apoptosis signaling pathways, leading to the occurrence of endoplasmic reticulum stress (ERS). Excessive ERS eventually leads to apoptosis, which is involved in the occurrence and development of cardiovascular diseases and is an important factor affecting the occurrence and development of heart failure. Moderate ERS enables cells to adapt to changes in the environment, restores normal endoplasmic reticulum function, and prevents heart failure; sustained and severe ERS triggers endoplasmic reticulum-mediated apoptosis, causing the myocardium to shift from compensation to failure, which is an important molecular mechanism of heart failure [8].

SIRT1 is mainly distributed throughout the cytoplasm and nucleus in cardiomyocytes. This protein not only has important biological effects on cardiac development, myocardial growth and metabolism, apoptosis and aging [9] but also plays an important role in cardiovascular diseases [10], such as myocardial ischemia/reperfusion (I/R) injury and heart failure [11, 12]. SIRT1 is believed to be closely associated with the pathogenesis of heart failure and the regulation of cardiac electrical activity [13], and it has been proposed as a prognostic tool for myocardial infarction. Studies have shown that SIRT1 protects cardiomyocytes from ERS by interacting with and deacetylating eukaryotic translation initiation factor 2α (eIF2α) on Lys-141 (K141) and Lys-143 (K143) residues during stress-mediated injury.

[1]Department of Cardiology, Institute of Cardiovascular Development and Translational Medicine, The Second Affiliated Hospital of Wenzhou Medical University, Wenzhou 325027, China and [2]Department of Cardiology, The Affiliated Hospital of Youjiang Medical University for Nationalities, Baise 533000, China
Correspondence: Teng-fang Lai (ltf15907861037@163.com) or Lei Li (lileiii@hotmail.com)

Received: 12 July 2021 Accepted: 26 October 2021
Published online: 1 December 2021

Dapagliflozin (DAPA), a new type of sodium-glucose cotransporter 2 (SGLT2) inhibitor, is an oral hypoglycemic drug that reduces glucose reabsorption by the kidneys and increases glucose excretion in urine [14]. In addition to lowering blood sugar, DAPA also plays an important role in cardiovascular disease [15]. It has been indicated to significantly reduce cardiovascular events and heart failure hospitalization rates of patients with type 2 diabetes mellitus (T2DM) [16]. Studies have shown that SGLT2 can reduce inflammation and the ERS response [17]. In addition, DAPA improves insulin resistance and increases the expression of SIRT1 protein induced by a high-fat diet [18]. DAPA can reduce cardiac remodeling in mouse models of cardiac pressure overload [19], and acute DAPA administration after cardiac ischemia can reduce cardiac dysfunction in rats with cardiac I/R injury [20]. However, whether DAPA inhibits ERS by activating the protein expression of SIRT1 to exert a protective effect on heart failure has never been studied. Inhibiting apoptosis can improve pressure overload-induced myocardial remodeling. These findings indicate that DAPA inhibits ERS-induced apoptosis by activating SIRT1, thereby improving myocardial remodeling in heart failure patients.

MATERIALS AND METHODS

Reagents and antibodies

Thapsigargin (TG), EX527, and DAPA were purchased from Glpbio (Montclair, CA, USA), and human angiotensin II (Ang II) was purchased from MedChemExpress (Shanghai, China). Antibodies against PERK (3192), p-PERK (15033), eIF2α (5324), p-eIF2α (3398), cleaved caspase 3 (9664), GRP78 (3177), CHOP (2895), and tubulin (2128) were purchased from Cell Signaling Technology. Antibodies against Bax (ab32503), ATF4 (ab23760) and Bcl-2 (ab59348) were purchased from Abcam (United Kingdom). Annexin V-FITC/PI was obtained from Beyotime Institute of Biotechnology. HL-1 cells and mouse cardiac fibroblasts (MCFs) were obtained from the China Cell Line Bank (Shanghai, China) and maintained as described previously.

Animals

Male C57BL/6 mice (6–8 weeks old) were purchased from the Animal Center of Wenzhou Medical University. All mice were housed with an alternating day/night cycle of 12/12 h, with a temperature of 23 ± 3 °C and humidity of 50% ± 5% and free access to food and water. Animal use and care procedures complied with the National Institutes of Health's Guide for the Care and Use of Laboratory Animals. This study was approved by the Animal Protection and Ethics Committee of Wenzhou Medical University (No: wydw2020-0667).

Cell scratch

Three parallel lines were drawn on the bottom of each well of a six-well plate in advance, and the digested fibroblasts were seeded evenly in the 6-well plate and incubated for 24 h in a carbon dioxide incubator. Then, three parallel lines were drawn perpendicular to the parallel line at the bottom of the six-well plate with a 200 μL pipette tip, and the cells were cultured in a carbon dioxide incubator. The six-well plate was photographed under an inverted microscope at 0 and 12 h. The speed of cell migration was observed.

Transwell assay

The fibroblasts were digested, counted and prepared at a concentration of 5×10^5/mL. RPMI-1640 medium supplemented with 10% FBS was added to the 24-well plate, the chambers were placed into the wells of the 24-well plate, 200 μL of the cell suspension was added to the chamber, and the treatments were added to the compartment. The 24-well plate was cultured in a carbon dioxide incubator for 12 h, and the chambers were then removed, fixed with 4% paraformaldehyde for 30 min, and stained with crystal violet for 15 min. After washing away the excess crystal violet, the chambers were placed into a 24-well plate and observed and photographed under an inverted microscope.

Flow cytometry

HL-1 cells were digested with EDTA-free trypsin, centrifuged at 1000 r/min for 5 min, resuspended in PBS, and incubated with 5 μL of Annexin V-FITC at room temperature for 10 min. Then, 5 μL of PI was added to 100 μL of (1×10^5) HL-1 cells at room temperature. Apoptosis was analyzed by flow cytometry.

TUNEL staining

The mouse heart was placed in O.C.T., and the blocks were then frozen at −80 °C and sliced into 5 μm-thick sections with a frozen slicer. After placing the sections at room temperature for 20 min, the frozen sections were washed three times with PBS for 5 min each time. The tissue sections were fixed with 4% paraformaldehyde for 30 min and permeabilized with 0.3% PBS-Triton X-100 for 10 min. Then, the sections were stained with TUNEL (Roche, Mannheim) according to the kit instructions to analyze cardiomyocyte apoptosis. After the tissue was incubated with DAPI in the dark for 10 min, the images were observed under a microscope.

WGA

The mouse heart was placed in O.C.T., and the blocks were then frozen at −80 °C and sliced with a frozen slicing instrument. After the sections were placed at room temperature for 20 min, the frozen sections were washed with PBS three times for 5 min each time. WGA was added to the frozen heart sections, followed by incubation for 10 min at room temperature. The sections were observed with a positive microscope.

Immunofluorescence staining

The cells were fixed with 4% paraformaldehyde, permeabilized with 0.3% PBS-Triton X-100 for 10 min, and sealed with 5% BSA at 37 °C for 1 h. Then, the cells were incubated with CHOP (L63F7) (1:100, cat# 2895, Cell Signaling Technology) overnight at 4 °C, after which the cells were incubated with AlexaFluor® 488 goat anti-mouse secondary (cat# ab150117, Abcam) and phalloidin-iFluor 594 (1:100, cat# ab176757, Abcam) secondary antibodies at room temperature for 1 h. Finally, the cells were incubated at room temperature in the dark. After the cells were incubated with DAPI in the dark for 10 min, the cells were observed and photographed with a fluorescence microscope.

Real-time quantitative PCR

Total RNA was extracted from cells and heart tissues with TRIzol reagent (Invitrogen, Carlsbad, CA, USA). RNA was reverse-transcribed using a ReverTra Ace Qpcr RT Kit (Toyobo, Shanghai, China). RT-PCR was performed with IQ SYBR Green Supermix (Bio-Rad, Hercules, CA, USA). GAPDH was used as the housekeeping gene. The relative gene expression level of each target gene was calculated by the $2^{-\Delta\Delta CT}$ method.

Western blotting

Total proteins were extracted from heart tissue and cells, purified, and quantified by the BCA method. Cellular proteins (20 μg) and tissue protein (40 μg) were separated by polyacrylamide gel electrophoresis and transferred to PVDF membranes (Thermo Fisher, Waltham, MA, USA). The membranes were sealed with 5% skim milk for 2 h at room temperature and then incubated overnight with the corresponding primary antibodies at 4 °C, including anti-SIRT1 (1:1000, cat# A11267, ABclonal), anti-PERK (C33E10) (1:1000, cat# 3192, Cell Signaling Technology), anti-p-PERK (Thr980) (1:1000, cat# MA5-15033, Invitrogen), anti-ATF4 (1:1000, cat# ab23760, Abcam), anti-GRP78 (C50B12) (1:1000, cat# 3177, Cell Signaling Technology), anti-eIF2α (D7D3) (1:1000, cat#

5324, Cell Signaling Technology), anti-p-eIF2α (Ser51) (D9G8) (1:1000, cat# 3398, Cell Signaling Technology), anti-CHOP (L63F7) (1:1000, cat# 2895, Cell Signaling Technology), and anti-cleaved Caspase 3 (Asp175) (1:1000, cat# 9664, Cell Signaling Technology). The next day, the membranes were incubated with the corresponding secondary antibodies (mouse or rabbit antibodies, 1:5000, Cell Signaling Technology) at room temperature for 2 h. The signal was visualized using a ChemiDoc™ XRS+ system and Image Lab software (Bio-Rad).

Mouse model

The mice were anesthetized with 1.5% isoflurane, fixed on a constant temperature pad, and connected to a small animal ventilator through endotracheal intubation. The chest cavity was opened in front of the sternum, and the aortic arch was exposed and pierced with a 6-0 nylon suture between the left common carotid artery and the brachiocephalic trunk. A 27 G coarctation needle was placed close to the blood vessel and inserted into the artery, and the coarctation needle was ligated with nylon suture. Then, the coarctation needle was quickly removed, and the chest was closed and sutured. The incision was coated with iodophor, and the ventilator was disconnected after the mice resumed spontaneous breathing. The 6-0 nylon suture was passed through the artery in the sham operation group and DAPA group without ligation, and the rest of the operation was the same as that in the model group.

The mice were randomly divided into four groups: (1) a sham-operated group (daily oral gavage with 0.5 mL 0.9% normal saline); (2) a DAPA group (daily oral gavage with 0.5 mL of DAPA (1 mg/kg) from the time of the sham operation to 4 weeks after the operation); (3) a TAC group (daily oral gavage with 0.5 mL of 0.9% normal saline from the time of the operation to 4 weeks after the operation); and (4) a TAC + DAPA-treated group (daily oral gavage with 0.5 mL of DAPA (1 mg/kg) from the time of the operation to 4 weeks after the operation).

Myocardial histopathology

To evaluate cardiac morphological changes and the degree of myocardial fibrosis in mice after 4 weeks of pressure overload, the hearts of mice in each group were removed, washed with normal saline and fixed in a 4% paraformaldehyde solution overnight. The fixed hearts were embedded in wax blocks and cut into 5 μm-thick sections with a paraffin slicer. The paraffin sections were heated for 2 h before being stained and dewaxed, and hematoxylin and eosin (HE) staining and Masson's trichromatic staining were then performed according to the kit instructions, after which the samples were observed under a fluorescence microscope (Olympus BX51, Tokyo, Japan).

Statistical analysis

SPSS 22 software was used to perform statistical analysis, and all data are expressed as the means ± SD. Comparisons between experimental groups were conducted using Student's *t* test, and $P < 0.05$ was considered statistically significant.

RESULTS

Dapagliflozin can improve the survival rate and heart function and reduce oxidative stress in mice with pressure overload

Four weeks after transverse aortic constriction (TAC), all mice in the sham operation and DAPA groups survived, while the survival rates in the TAC and TAC + DAPA groups were 61% and 74%, respectively (Fig. 1a), indicating that the survival rates of mice with heart failure were improved after DAPA treatment. Four weeks after pressure overload, the effect of DAPA on cardiac function was examined by echocardiography (Fig. 1b). The results confirmed that DAPA could improve the heart function of mice at 4 weeks after TAC; left ventricular ejection fraction (LVEF) and left ventricular fractional shortening (LVFS) in the TAC group were significantly lower than those in the sham operation group, while LVEF and LVFS in the TAC + DAPA group were significantly higher than those in the TAC group. Left ventricular internal diameter end diastole (LVIDd) and left ventricular posterior wall end diastole (LVPWd) were significantly higher than those in the sham operation group, while LVIDd and LVPWd were significantly lower in the TAC + DAPA group than in the TAC group (Fig. 1c, d, e, f). The heart weight/body weight (HW/BW) and the left ventricular/body weight (LW/BW) ratios in the TAC group were higher than those in the sham operation group. The HW/BW and LW/BW decreased significantly after DAPA treatment (Fig. 1g and h).

Dapagliflozin can reduce pressure overload-induced cardiac hypertrophy and fibrosis in mice

Compared with that in the sham and DAPA groups, at 4 weeks after TAC surgery, morphological analysis confirmed that DAPA could improve hypertrophy in TAC mice. The HE and WGA staining results showed that the size of cardiomyocytes increased significantly after TAC surgery (Fig. 2a and b), and there was overproduction of ANP, BNP and α-MHC (Fig. 2d). DAPA treatment significantly reduced these pathological changes caused by pressure overload (Fig. 2a, b, d). Cardiac fibrosis is an integrated process in the development of pathological cardiac hypertrophy. In this study, compared with the sham and DAPA groups, the TAC group exhibited significant interstitial and perivascular fibrosis (Fig. 2a and c); however, DAPA treatment significantly reduced cardiac fibrosis compared with TAC and suppressed the expression of fibrosis-related markers (Fig. 2e). Persistent cardiac hypertrophy and fibrosis directly led to cardiac insufficiency and heart failure.

Dapagliflozin reduces Ang II-induced hypertrophy in vitro

To examine whether DAPA has an inhibitory effect on cardiomyocytes, we treated cardiomyocytes with 100 nM Ang II. DAPA treatment inhibited Ang II-induced cardiomyocyte hypertrophy, which was reflected in the reduced cell surface area (Fig. 3a and b). The mRNA expression of the embryonic genes ANP and BNP was significantly reduced (Fig. 3c).

Dapagliflozin inhibits fibroblast migration

To confirm whether DAPA inhibits fibrosis, we treated MCFs with 100 nM Ang II. The Transwell and cell scratch results showed that after Ang II stimulation, DAPA significantly inhibited the conversion of fibroblasts to myofibroblasts (Fig. 4a–d). Fibroblast migration was weakened, and the mRNA expression of the fibrosis genes α-SMA, collagen I, and collagen III was significantly weakened (Fig. 4e, f).

Dapagliflozin can inhibit Ang II-induced cardiomyocyte apoptosis and endoplasmic reticulum stress

To examine whether DAPA has an antiapoptotic effect on cardiomyocytes, we treated cardiomyocytes with 100 nM Ang II. The flow cytometry results showed that the apoptotic rate of cardiomyocytes was significantly increased after Ang II stimulation, and this effect was reversed by DAPA treatment (Fig. 5c and d). The Western blot results showed that DAPA downregulated the levels of cleaved caspase 3 and Bax and upregulated the expression level of Bcl-2 compared with those in the Ang II group (Fig. 5a and b). These results indicate that DAPA may play a protective role against Ang II-induced cardiomyocyte apoptosis. Furthermore, Ang II stimulation of cardiomyocytes activated ERS, as indicated by significant increases in the ERS proteins p-perk, p-eIF2α, CHOP, GRP78 and ATF4, while DAPA treatment reduced the expression of the ERS proteins CHOP, GRP78 and ATF4 (Fig. 5e–k), indicating that DAPA can inhibit ERS in Ang II-induced cardiomyocytes.

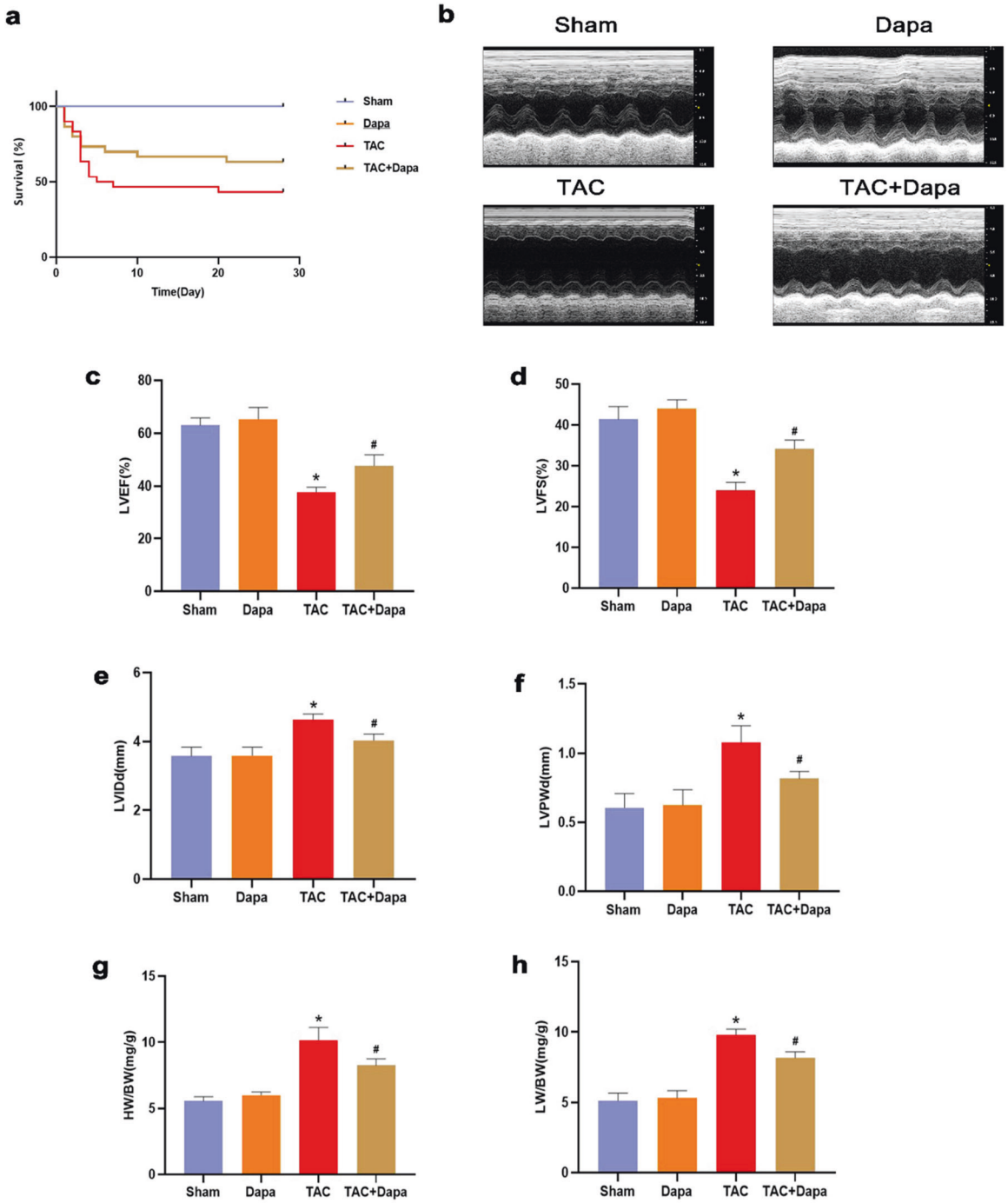

Fig. 1 The effects of DAPA on the survival rate of mice and heart function associated with cardiac hypertrophy. a The survival rate of mice in the DAPA-treated group compared with the TAC group. **b** Representative echocardiographic images of each group. **c**–**f** Echocardiographic parameters, including left ventricular ejection fraction (LVEF), left ventricle fractional shortening (LVFS), left ventricular internal diameter (LVID), left ventricular posterior wall thickness (LVPW), of each group. **g**, **h** Statistical results of heart weight/body weight (HW/BW) and left ventricular/body weight (LW/BW). $n = 6$, $^{*}P < 0.05$ versus the sham or DAPA group, $^{\#}P < 0.05$ versus the TAC.

Dapagliflozin can inhibit Ang II-induced endoplasmic reticulum stress to inhibit cardiomyocyte apoptosis

To further explore whether ERS is associated with the protective effect of DAPA on cardiomyocytes after Ang II stimulation, TG was used to activate ERS in cardiomyocytes. The Western blot results showed that compared with those in the DAPA + Ang II group, TG treatment significantly increased the levels of p-perk, p-eIF2α, CHOP, GRP78 and ATF4 (Fig. 6e–k). In addition, immunofluorescence staining of CHOP showed that TG promoted ERS activity (Fig. 6c and d). As mentioned previously, DAPA protected cardiomyocytes against Ang II-induced ERS. To confirm whether the DAPA-induced inhibition of ERS attenuates Ang II-induced apoptosis, we used TG to activate ERS and measured the levels of apoptosis biomarkers, including Bcl-2, cleaved caspase 3, and Bax (Fig. 6a and b). The results showed that TG inhibited the antiapoptotic effect of DAPA. Therefore, DAPA reduces Ang II-induced cardiomyocyte apoptosis by inhibiting ERS.

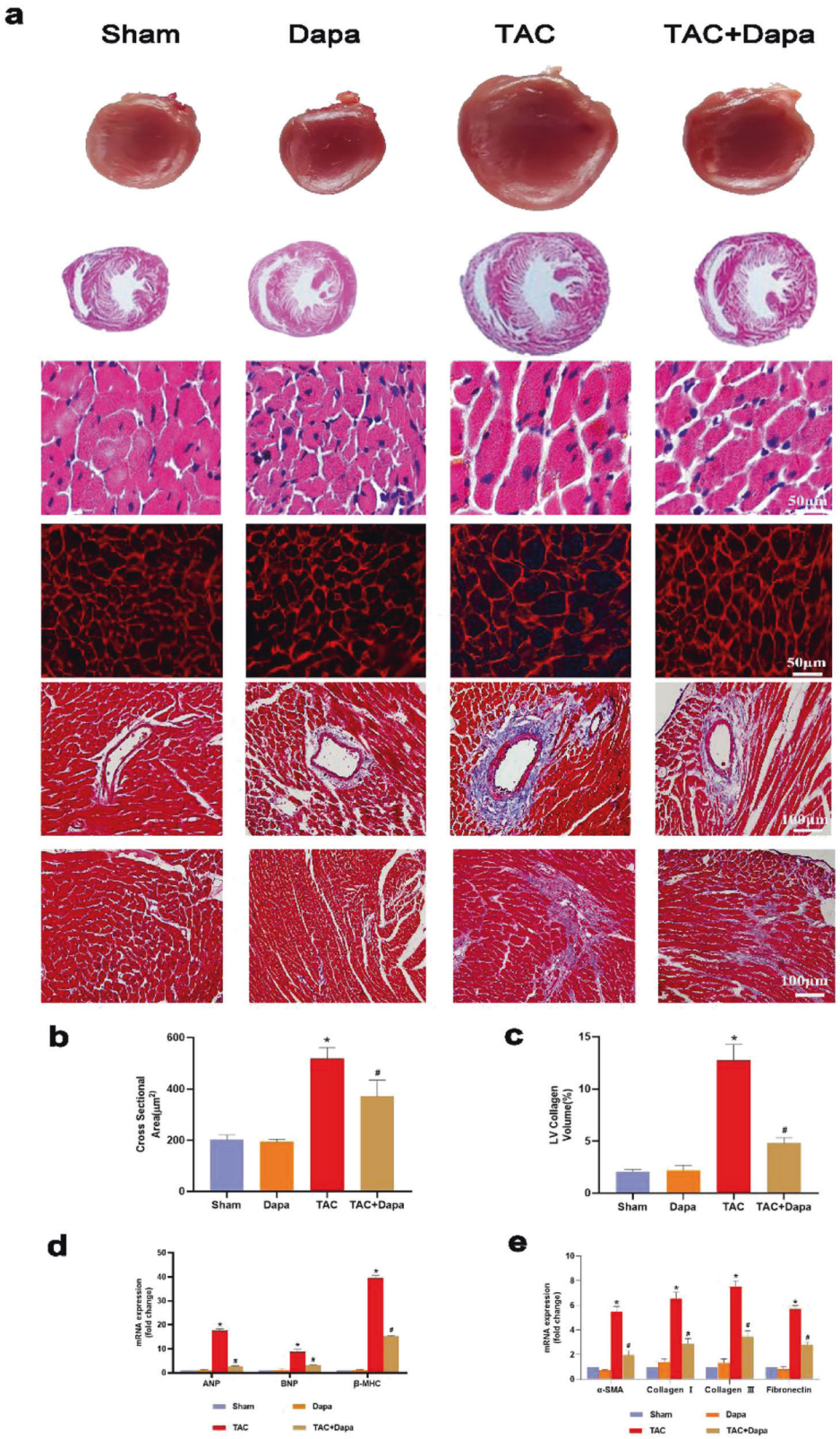

Fig. 2 Effect of treatment with dapagliflozin (DAPA) on transverse aortic constriction (TAC)-induced cardiac hypertrophy in mice. a Representative images of the morphological analysis of cardiac hypertrophy as reflected by the whole heart and heart short-axis cross-section (top), hematoxylin and eosin (H&E) staining (middle), fluorescein isothiocyanate-labeled wheat germ agglutinin (WGA) staining (middle), and Masson's trichrome (MASSON) staining (bottom). **b** Statistical data of the cardiomyocyte cross-sectional areas. **c** LV collagen ratio in interstitial fibrosis. **d** ANP, BNP and β-MHC mRNA levels were assessed by real-time PCR. **e** α-SMA, collagen I, collagen III and fibronectin mRNA levels were determined by real-time PCR. $n = 6$, $^{*}P < 0.05$ versus the sham or DAPA group, $^{\#}P < 0.05$ versus the TAC group.

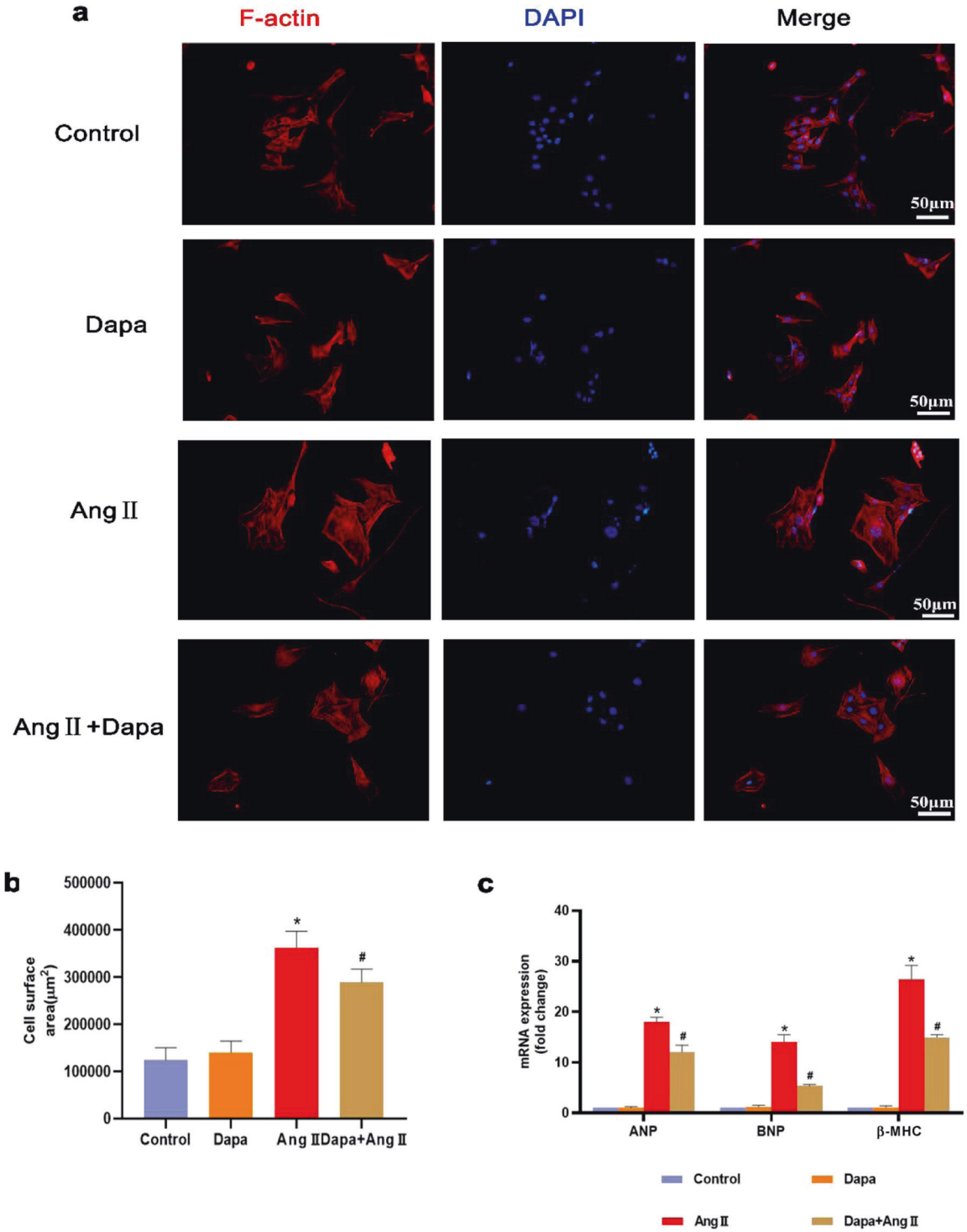

Fig. 3 DAPA attenuated Ang II-induced cardiac hypertrophy in vitro. a The cell surface area of HL-1 cells was assessed by TRITC-conjugated phalloidin staining. **b** Calculated cell surface area (>100 cells per group). **c** ANP, BNP and β-MHC mRNA levels were assessed by real-time PCR. $n = 6$, $^{*}P < 0.05$ versus the CON or DAPA group, $^{\#}P < 005$ versus the Ang II.

Dapagliflozin inhibits Ang II-induced endoplasmic reticulum stress by activating SIRT1 and reduces cardiomyocyte apoptosis

To evaluate the role of SIRT1 and ERS activation in Ang II-induced cardiomyocyte apoptosis, we used the known SIRT1 inhibitor EX527. The experimental results showed that in the EX527 + DAPA + Ang II group, cleaved caspase-3 and Bax levels increased, and the expression level of Bcl-2 decreased (Fig. 7a and b). These results indicate that SIRT1 inhibition is associated with Ang II-induced cardiomyocyte apoptosis. However, the relationship between SIRT1 and the PERK-eIF2α-CHOP pathway remains unclear. Therefore, we used EX527 to inhibit SIRT1 expression in cardiomyocytes. In the presence of EX527, the SIRT1 protein level in Ang II-stimulated cardiomyocytes decreased, and the p-PERK and p-eIF2α protein levels decreased after DAPA treatment (Fig. 7e–k). The CHOP immunofluorescence staining results were consistent with the Western blot results (Fig. 7c and d). Our data

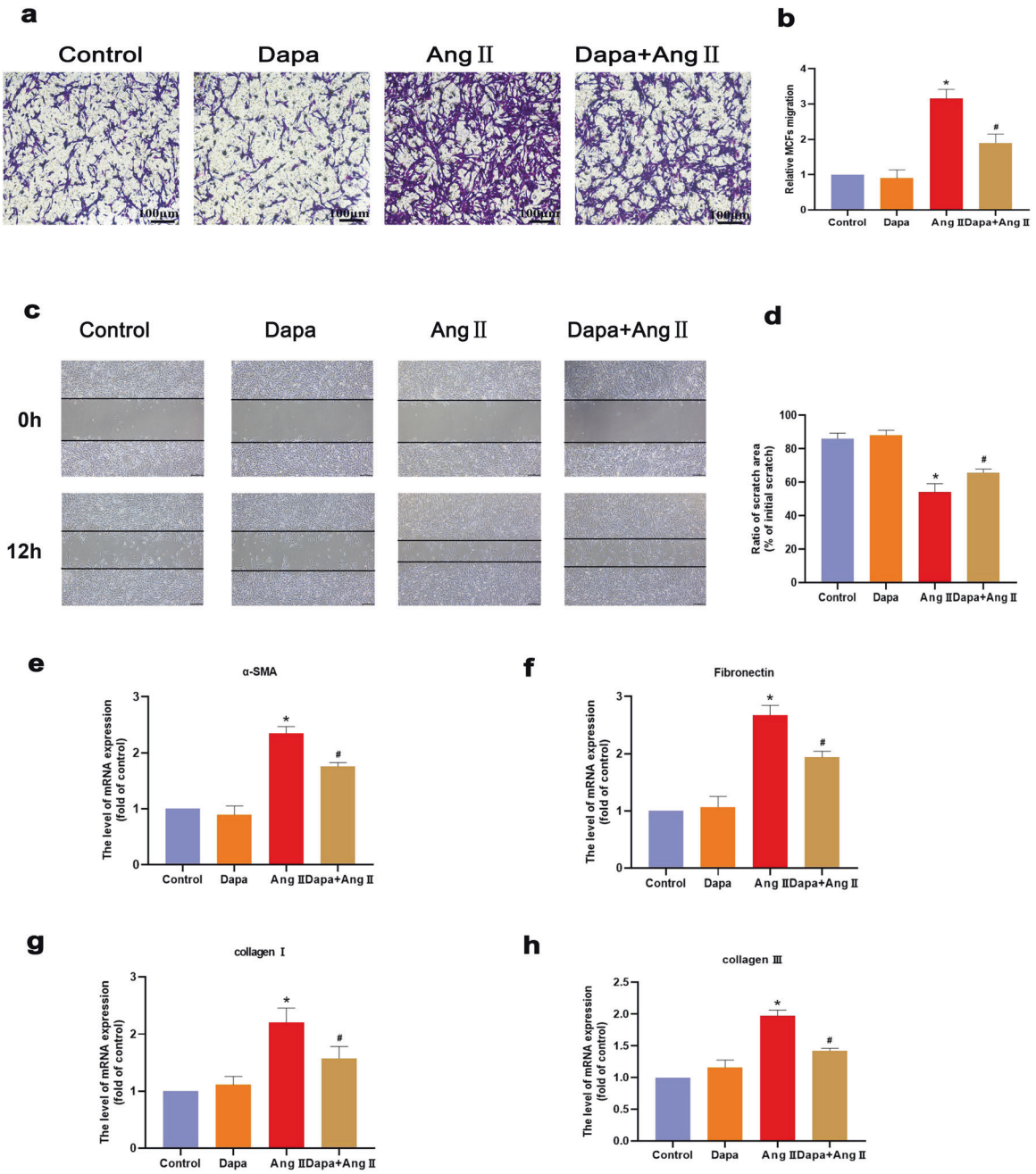

Fig. 4 DAPA inhibits the transformation of cardiac fibroblasts into cardiac myofibroblasts by Ang. a, **b** Transwell chamber experiment was used to analyze the cell migration ability force. **c**, **d** Cell scratch test to analyze cell migration ability. **e**–**h** α-SMA, fibronectin, collagen III, collagen I and fibronectin mRNA levels were detected by real-time PCR. $n = 6$, $^{*}P < 0.05$ versus the CON or DAPA group, $^{\#}P < 0.05$ versus the Ang II group.

indicate that SIRT1 can inhibit ERS in cardiomyocytes by inhibiting the PERK-eIF2α-CHOP pathway.

Dapagliflozin reduces pressure overload-induced endoplasmic reticulum stress and apoptosis in mice

To explore the protective effect of DAPA on pressure-overloaded mice, a TAC mouse model was established, and the mice were intragastrically administered DAPA at a dose of 1 $mg{\cdot}kg^{-1}{\cdot}d^{-1}$ for 4 weeks. TUNEL staining showed that compared with that of the sham operation group, the number of apoptotic cardiomyocytes in the TAC group was significantly increased (Fig. 8c and d). The Western blot results showed that DAPA significantly reduced the levels of cleaved caspase 3 and Bax in mouse hearts (Fig. 8a and b) and increased the expression of SIRT1 and reduced ERS proteins (Fig. 8e–k). These results indicate that DAPA can inhibit ERS and has a significant antiapoptotic effect, which is consistent with the in vitro results.

DISCUSSION

Cardiomyocyte apoptosis plays an important role in the occurrence and development of heart failure. In a failing heart, a small amount of persistent cardiomyocyte death can be observed [21]. Cardiomyocytes are highly differentiated cells, and cardiomyocyte death can lead to permanent loss of myocardial contractile proteins and fatal heart failure [22–24]. Therefore, a small but

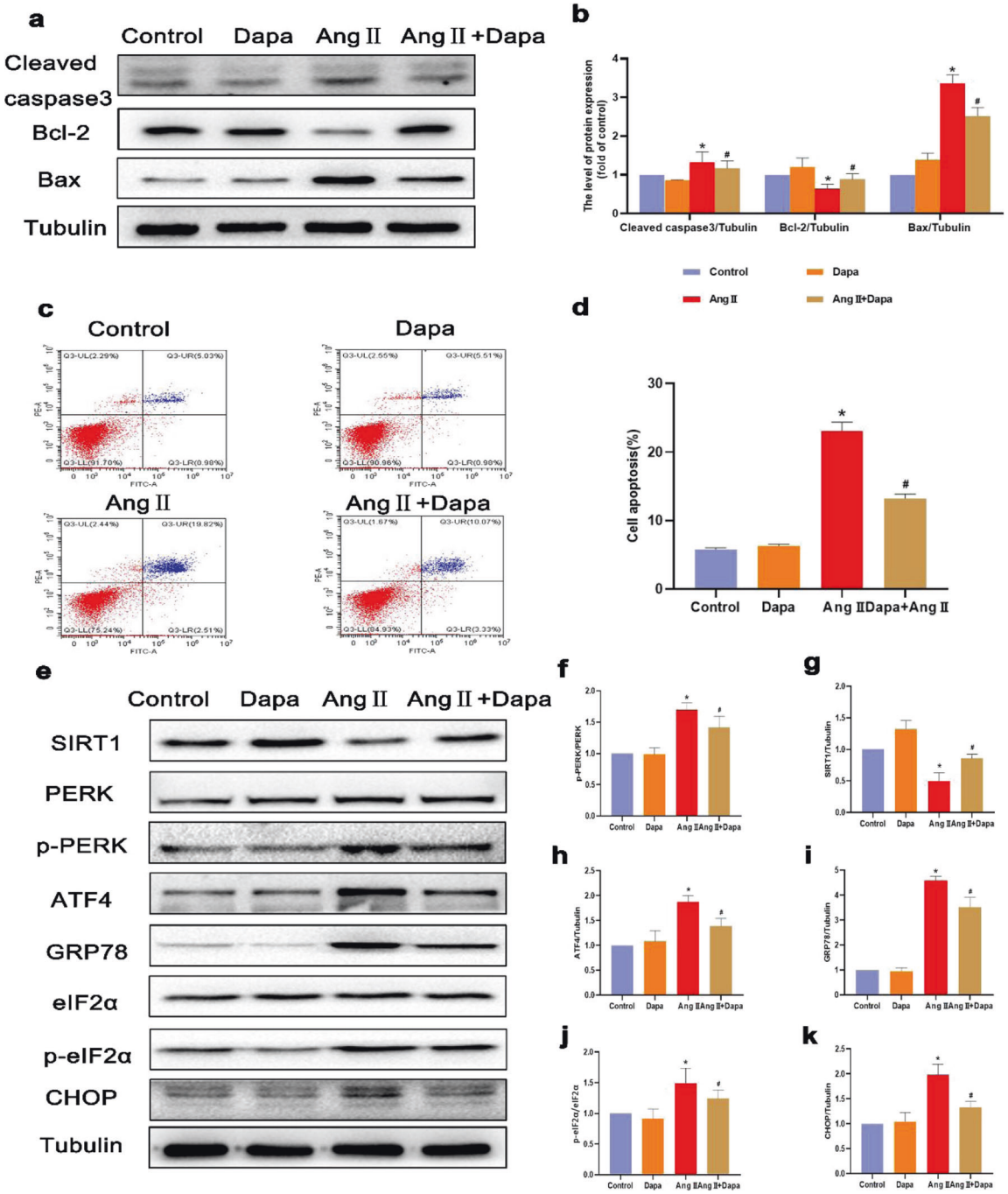

Fig. 5 DAPA inhibited chondrocyte apoptosis in Ang II-stimulated cardiomyocytes. a, **b** The protein levels of Bcl-2, Bax, and cleaved caspase 3 in each group were determined. **c**, **d** Flow cytometry was used to assess the apoptosis of cardiomyocytes labeled with Annexin V and PI fluorescence. **e**–**k** The protein expression levels and optical density analysis of SIRT1, p-PERK, ATF4, GRP-78, p-eIF2α, and CHOP in the myocardium. $n = 6$, $^{*}P < 0.05$ versus the CON or DAPA group, $^{\#}P < 0.05$ versus the Ang II.

sustained amount of cardiomyocyte apoptosis can lead to fatal heart failure [25]. The inhibition of cardiomyocyte apoptosis through drugs or nondrug treatments can significantly slow ventricular remodeling and improve cardiac function [26–29]. We measured the protein expression levels of Bax and Bcl-2, and the results showed that DAPA could significantly inhibit TAC-induced cardiomyocyte apoptosis. The TUNEL staining results were the same as the Western blot results, which further proved that DAPA could reduce cardiac apoptosis caused by pressure loading in mice.

CHOP and GRP78 are typical biomarkers of ERS [30]. Studies have shown that CHOP-mediated cardiomyocyte apoptosis plays an important role in aortic coarctation model mice [31]. Our results showed that DAPA (10 μM) significantly reduced the expression levels of CHOP and GRP78, indicating that DAPA inhibited ERS caused by heart failure. In eukaryotic cells, ERS is mediated by three branches of the unfolded protein response, including PERK, IRE1α, and ATF6 [32]. Studies have shown that ERS is closely associated with heart failure, and ERS-related cardiomyocyte apoptosis occurs throughout the occurrence and development of myocardial remodeling [33].

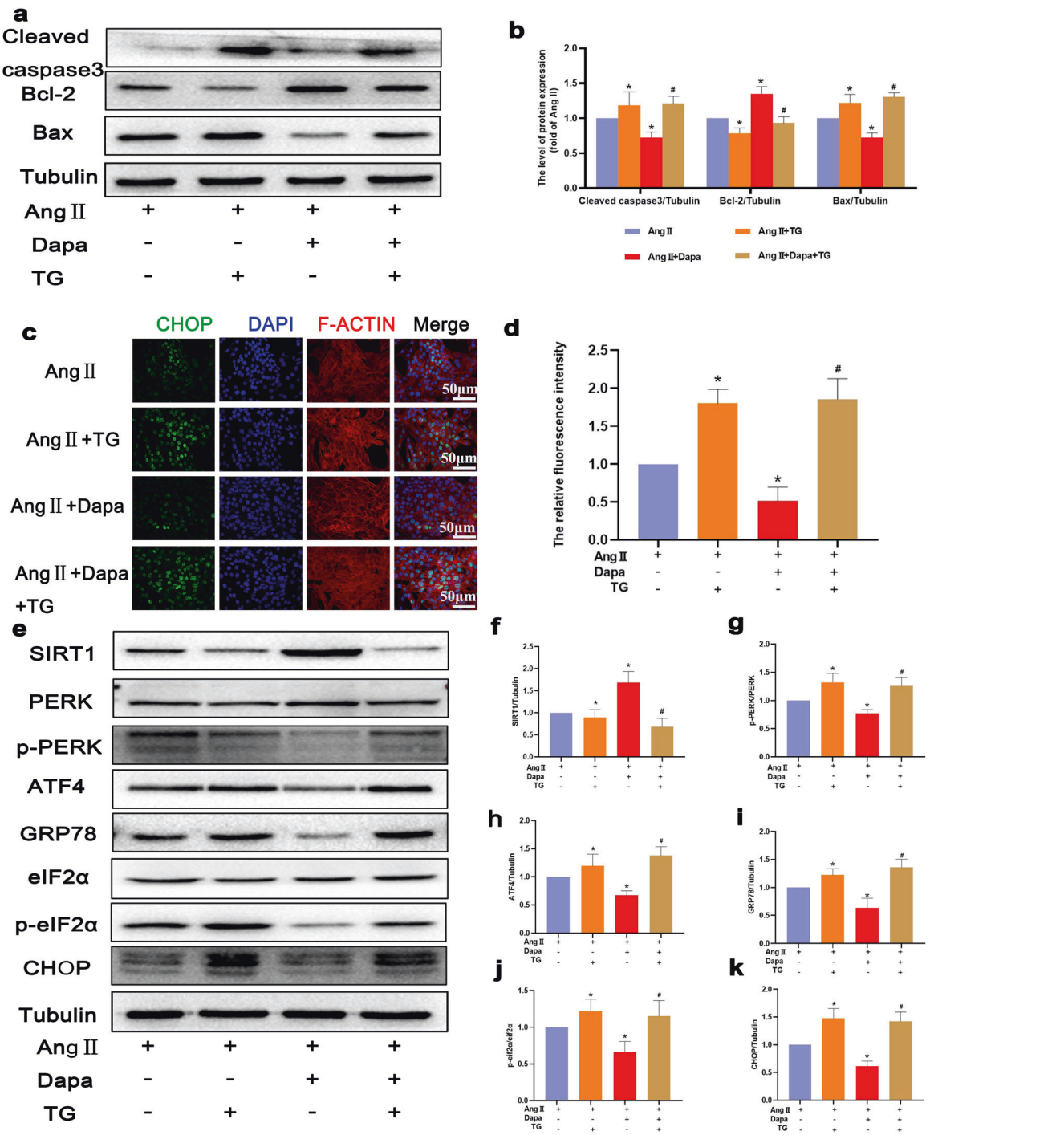

Fig. 6 DAPA inhibited ER stress in Ang II-induced cardiomyocytes. a, **b** The protein levels of Bcl-2, Bax, and cleaved caspase 3 in each group were detected. **c** CHOP immunofluorescence staining. Markedly increased green bright puncta indicated the upregulated expression of CHOP. **d** Quantification of the number of CHOP-positive chondrocytes in each group based on immunofluorescence staining. **e**–**k** The protein expression levels and optical density analysis of SIRT1, p-PERK, ATF4, GRP-78, p-eIF2α, and CHOP in the myocardium. $n = 6$, $^{*}P < 0.05$ versus the Ang II or Ang II + TG group, $^{\#}P < 0.05$ versus the Ang II + DAPA group.

In diabetic nephropathy, DAPA inhibits ERS-mediated apoptosis by inhibiting the eIF2α-ATF4-CHOP pathway in vitro and in vivo [34]. In this study, we found for the first time that DAPA could inhibit ERS-mediated apoptosis in heart failure by inhibiting the eIF2α-ATF4-CHOP pathway, revealing the relationship between ERS and cardiomyocyte apoptosis. To examine this relationship, we used the classic ERS inducer TG. We found that the antiapoptotic effect of DAPA was reversed by TG treatment. This study demonstrated for the first time that the protective effect of DAPA is associated with inhibition of the PERK-eIF2α-ATF4-CHOP signaling pathway, which directly inhibits CHOP expression in cardiomyocytes and subsequent apoptosis activation. However, it is unclear whether the other two ERS pathways are associated with the protective effect of DAPA on TAC, and further research is needed.

Several studies have confirmed that SIRT1 can protect the heart by inhibiting ERS-related apoptosis [35]. A recent study by

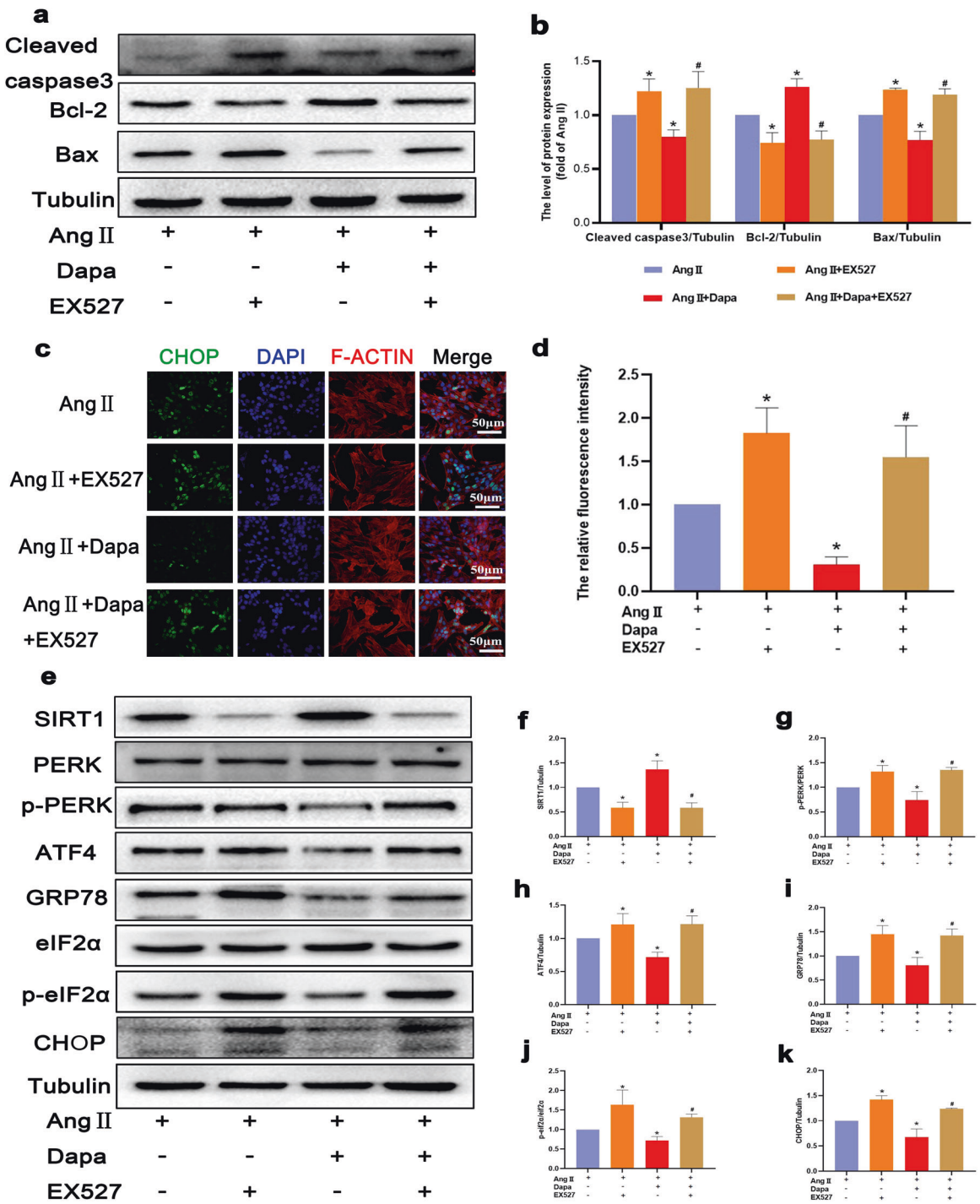

Fig. 7 EX527 abrogated the inhibitory effect of DAPA on Ang II-induced ER stress in cardiomyocytes. a, **b** The protein levels of Bcl-2, Bax, and cleaved caspase 3 in each group were detected. **c** CHOP immunofluorescence staining. Markedly increased green bright puncta indicated the upregulated expression of CHOP. **d** Quantification of the number of CHOP-positive chondrocytes in each group based on immunofluorescence staining. **e**–**k** The protein expression levels and optical density analysis of SIRT1, p-PERK, ATF4, GRP-78, p-eIF2α, and CHOP in the myocardium. $n = 6$, $^{*}P < 0.05$ versus the Ang II or Ang II + EX527 group, $^{\#}P < 0.05$ versus the Ang II + DAPA group.

Prola A et al. demonstrated that SIRT1 inhibits ERS by inhibiting the PERK-eIF2α-ATF4 ERS pathway, which ultimately reduces ERS-induced apoptosis [36]. Our results show for the first time that Ang II treatment reduces SIRT1 expression and that DAPA can reverse this effect. In addition, SIRT1 was activated in the hearts of TAC mice after DAPA treatment and heart function was improved by DAPA in TAC mice. Furthermore, we found that DAPA treatment could significantly reduce the expression levels of ERS and apoptotic proteins in cardiomyocytes stimulated by Ang II, suggesting that DAPA can reduce ERS and inhibit

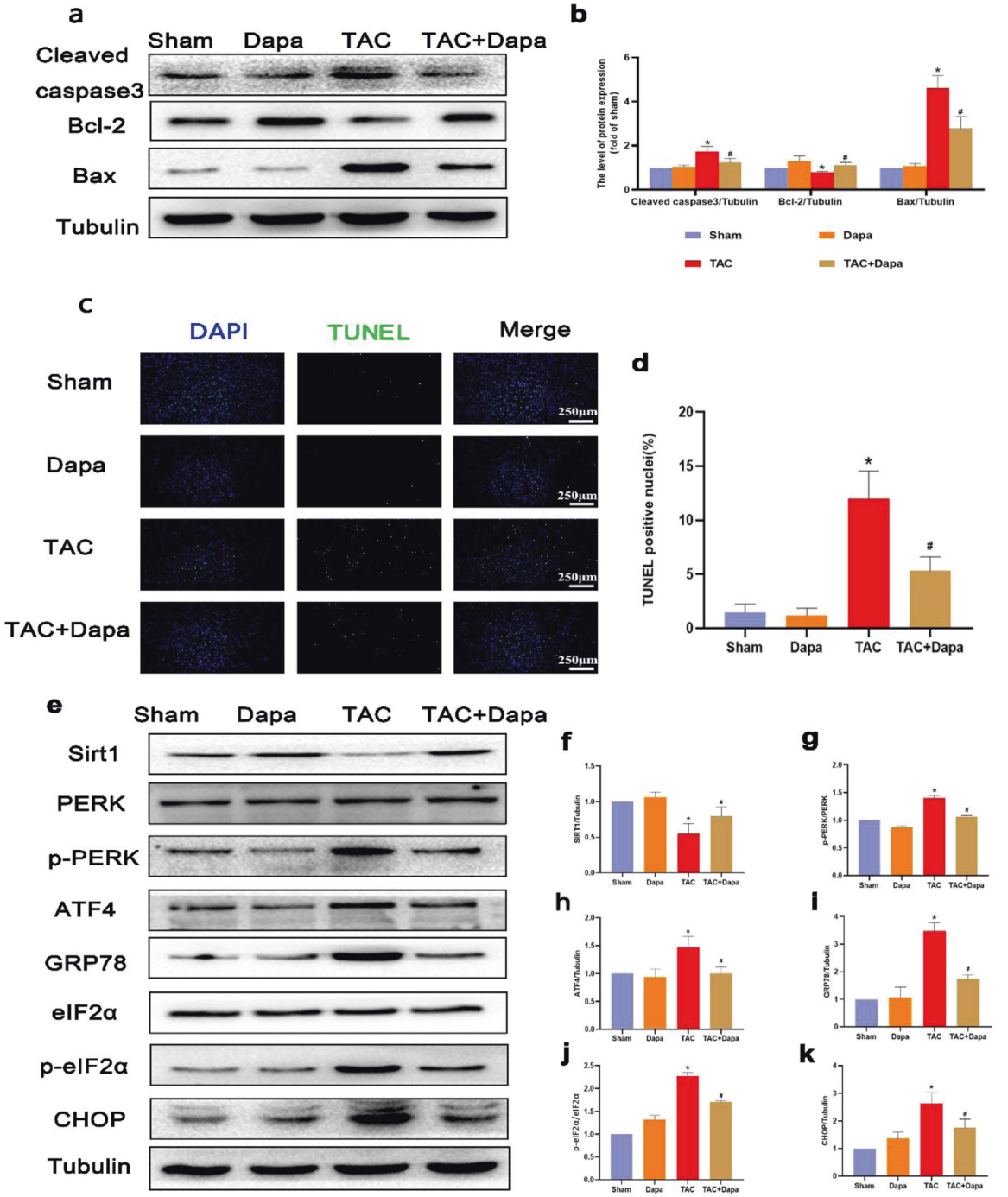

Fig. 8 DAPA inhibited cardiomyocyte apoptosis and ER stress in the TAC model. a, **b** The protein levels of Bcl-2, Bax, and cleaved caspase 3 in each group were determined. **c**, **d** TUNEL staining of apoptotic cardiomyocytes and quantification of TUNEL staining in each group. **e**–**k** The protein expression levels and optical density analysis of SIRT1, p-PERK, ATF4, GRP-78, p-eIF2α, and CHOP in the myocardium. $n = 6$, $^{*}P < 0.05$ versus the sham or DAPA group, $^{\#}P < 0.05$ versus the TAC.

cardiomyocyte apoptosis. After the administration of the SIRT1 inhibitor EX527, the protective effect of DAPA on cardiomyocytes was blocked. These results showed that the important effect of SIRT1 on Ang II-induced cardiomyocyte apoptosis was associated with inhibition of the PERK-eIF2α-ATF4-CHOP pathway. In summary, our study shows for the first time that DAPA can inhibit PERK-eIF2α-ATF4-CHOP by promoting SIRT1 expression in Ang II cardiomyocytes to reduce cardiomyocyte apoptosis. Similarly, it is unclear whether the other two ERS pathways are associated with SIRT1 expression and the protective effect of DAPA on TAC, which requires further study.

In conclusion, the current study proved, for the first time, that DAPA can improve the progression of heart failure by inhibiting ERS and reducing cardiomyocyte apoptosis. DAPA inhibits the PERK-eIF2α-ATF4-CHOP signaling pathway in the endoplasmic reticulum by promoting SIRT1 expression to protect cardiomyocytes against apoptosis.

ACKNOWLEDGEMENTS

This study was supported by a grant from the National Natural Science Foundation of China (81770292) and Key Projects of Workstation of He Lin (18331101) and Wenzhou Science and Technology Major Projects (2018ZY007)

AUTHOR CONTRIBUTIONS

LL, LTF, FFR designed the research, FFR wrote the paper. FFR, ZYX, YNJ, XG, and QYC conducted the experiments. All the authors analyzed the data, revised the paper, and approved the final paper.

ADDITIONAL INFORMATION

Supplementary information The online version contains supplementary material available at https://doi.org/10.1038/s41401-021-00805-2.

Competing interests: The authors declare no competing interests.

REFERENCES

1. Hill JA, Olson EN. Cardiac plasticity. N Engl J Med. 2008;358:1370–80.
2. Wang L, Wang J, Cretoiu D, Li G, Xiao J. Exercise-mediated regulation of autophagy in the cardiovascular system. J Sport Health Sci. 2020;9:203–10.
3. Abbate A, Toldo S, Marchetti C, Kron J, Van Tassell BW, Dinarello CA. Interleukin-1 and the inflammasome as therapeutic targets in cardiovascular disease. Circ Res. 2020;126:1260–80.
4. Lund LH, Savarese G. Global public health burden of heart failure. Cardiac Fail Rev. 2017;3:7–11.
5. Coeytaux RR, Williams JW, Gray RN, Wang A. Percutaneous heart valve replacement for aortic stenosis: state of the evidence. Ann Intern Med. 2010;153:314–24.
6. van Empel VP, Bertrand AT, Hofstra L, Crijns HJ, Doevendans PA, De Windt LJ. Myocyte apoptosis in heart failure. Cardiovasc Res. 2005;67:21–9.
7. Sadoshima J, Montagne O, Wang Q, Yang G, Warden J, Liu J, et al. The MEKK1-JNK pathway plays a protective role in pressure overload but does not mediate cardiac hypertrophy. J Clin Invest. 2002;110:271–9.
8. Lin JH, Li H, Yasumura D, Cohen HR, Zhang C, Panning B, et al. IRE1 signaling affects cell fate during the unfolded protein response. Science. 2007;318:944–9.
9. Sundaresan NR, Pillai VB, Gupta MP. Emerging roles of SIRT1 deacetylase in regulating cardiomyocyte survival and hypertrophy. J Mol Cell Cardiol. 2011;51:614–8.
10. Nadtochiy SM, Urciuoli W, Zhang J, Schafer X, Munger J, Brookes PS. Metabolomic profiling of the heart during acute ischemic preconditioning reveals a role for SIRT1 in rapid cardioprotective metabolic adaptation. J Mol Cell Cardiol. 2015;88:64–72.
11. Ding M, Lei J, Han H, Li W, Qu Y, Fu E, et al. SIRT1 protects against myocardial ischemia-reperfusion injury via activating eNOS in diabetic rats. Cardiovasc Diabetol. 2015;14:143.
12. Akkafa F, Halil Altiparmak I, Erkus ME, Aksoy N, Kaya C, Ozer A, et al. Reduced SIRT1 expression correlates with enhanced oxidative stress in compensated and decompensated heart failure. Redox Biol. 2015;6:169–73.
13. Vikram A, Lewarchik CM, Yoon JY, Naqvi A, Kumar S, Morgan GM, et al. Sirtuin 1 regulates cardiac electrical activity by deacetylating the cardiac sodium channel. Nat Med. 2017;23:361–7.
14. Vrhovac I, Balen Eror D, Klessen D, Burger C, Breljak D, Kraus O, et al. Localizations of Na^+-*D*-glucose cotransporters SGLT1 and SGLT2 in human kidney and of SGLT1 in human small intestine, liver, lung, and heart. Pflug Arch. 2015;467:1881–98.
15. Cowie MR, Fisher M. SGLT2 inhibitors: mechanisms of cardiovascular benefit beyond glycaemic control. Nat Rev Cardiol. 2020;17:761–72.
16. Yurista SR, Silljé H, Oberdorf-Maass SU, Schouten EM, Pavez Giani MG, Hillebrands JL, et al. Sodium-glucose co-transporter 2 inhibition with empagliflozin improves cardiac function in non-diabetic rats with left ventricular dysfunction after myocardial infarction. Eur J Heart Fail. 2019;21:862–73.
17. Jaikumkao K, Pongchaidecha A, Chueakula N, Thongnak LO, Wanchai K, Chatsudthipong V, et al. Dapagliflozin, a sodium-glucose co-transporter-2 inhibitor, slows the progression of renal complications through the suppression of renal inflammation, endoplasmic reticulum stress and apoptosis in prediabetic rats. Diabetes Obes Metab. 2018;20:2617–26.
18. Swe MT, Thongnak L, Jaikumkao K, Pongchaidecha A, Chatsudthipong V, Lungkaphin A. Dapagliflozin not only improves hepatic injury and pancreatic endoplasmic reticulum stress, but also induces hepatic gluconeogenic enzymes expression in obese rats. Clin Sci (Lond). 2019;133:2415–30.
19. Shi L, Zhu D, Wang S, Jiang A, Li F. Dapagliflozin attenuates cardiac remodeling in mice model of cardiac pressure overload. Am J Hypertens. 2019;32:452–9.
20. Lahnwong S, Palee S, Apaijai N, Sriwichaiin S, Kerdphoo S, Jaiwongkam T, et al. Acute dapagliflozin administration exerts cardioprotective effects in rats with cardiac ischemia/reperfusion injury. Cardiovasc Diabetol. 2020;19:91.
21. Kostin S, Pool L, Elsässer A, Hein S, Drexler HC, Arnon E, et al. Myocytes die by multiple mechanisms in failing human hearts. Circ Res. 2003;92:715–24.
22. Guo X, Zhang Y, Lu C, Qu F, Jiang X. Protective effect of hyperoside on heart failure rats via attenuating myocardial apoptosis and inducing autophagy. Biosci Biotechnol Biochem. 2020;84:714–24.
23. Whelan RS, Kaplinskiy V, Kitsis RN. Cell death in the pathogenesis of heart disease: mechanisms and significance. Annu Rev Physiol. 2010;72:19–44.
24. Wencker D, Chandra M, Nguyen K, Miao W, Garantziotis S, Factor SM, et al. A mechanistic role for cardiac myocyte apoptosis in heart failure. J Clin Invest. 2003;111:1497–504.
25. Razavi HM, Hamilton JA, Feng Q. Modulation of apoptosis by nitric oxide: implications in myocardial ischemia and heart failure. Pharmacol Ther. 2005;106:147–62.
26. Sin TK, Yu AP, Yung BY, Yip SP, Chan LW, Wong CS, et al. Modulating effect of SIRT1 activation induced by resveratrol on Foxo1-associated apoptotic signalling in senescent heart. J Physiol. 2014;592:2535–48.
27. Patten RD, Pourati I, Aronovitz MJ, Baur J, Celestin F, Chen X, et al. 17beta-estradiol reduces cardiomyocyte apoptosis in vivo and in vitro via activation of phospho-inositide-3 kinase/Akt signaling. Circ Res. 2004;95:692–9.
28. Patten RD, Denofrio D, El-Zaru M, Kakkar R, Saunders J, Celestin F, et al. Ventricular assist device therapy normalizes inducible nitric oxide synthase expression and reduces cardiomyocyte apoptosis in the failing human heart. J Am Coll Cardiol. 2005;45:1419–24.
29. Liu Q, Chen L, Liang X, Cao Y, Zhu X, Wang S, et al. Exercise attenuates angiotensin-induced muscle atrophy by targeting PPARgamma/miR-29b. J Sport Health Sci. 2021;S2095–2546;00067–3. https://doi.org/10.1016/j.jshs.2021.06.002.
30. Uehara Y, Hirose J, Yamabe S, Okamoto N, Okada T, Oyadomari S, et al. Endoplasmic reticulum stress-induced apoptosis contributes to articular cartilage degeneration via C/EBP homologous protein. Osteoarthr Cartil. 2014;22:1007–17.
31. Okada K, Minamino T, Tsukamoto Y, Liao Y, Tsukamoto O, Takashima S, et al. Prolonged endoplasmic reticulum stress in hypertrophic and failing heart after aortic constriction: possible contribution of endoplasmic reticulum stress to cardiac myocyte apoptosis. Circulation. 2004;110:705–12.
32. Hotamisligil GS. Endoplasmic reticulum stress and the inflammatory basis of metabolic disease. Cell. 2010;140:900–17.
33. Li Z, Guo J, Bian Y, Zhang M. Intermedin protects thapsigargininduced endoplasmic reticulum stress in cardiomyocytes by modulating protein kinase A and sarco/endoplasmic reticulum Ca^{2+}ATPase. Mol Med Rep. 2021;23:107. https://doi.org/10.3892/mmr.2020.11746.
34. Shibusawa R, Yamada E, Okada S, Nakajima Y, Bastie CC, Maeshima A, et al. Dapagliflozin rescues endoplasmic reticulum stress-mediated cell death. Sci Rep. 2019;9:9887.
35. Li YP, Wang SL, Liu B, Tang L, Kuang RR, Wang XB, et al. Sulforaphane prevents rat cardiomyocytes from hypoxia/reoxygenation injury in vitro via activating SIRT1 and subsequently inhibiting ER stress. Acta Pharmacol Sin. 2016;37:344–53.
36. Prola A, Pires Da Silva J, Guilbert A, Lecru L, Piquereau J, Ribeiro M, et al. SIRT1 protects the heart from ER stress-induced cell death through eIF2alpha deacetylation. Cell Death Differ. 2017;24:343–56.